Neurospine 2019;16(2):298-304.
https://doi.org/10.14245/ns.1836030.015

Neurospine
pISSN 2586-6583 eISSN 2586-6591

Original Article

Comparative Finite Element Analysis of Lumbar Cortical Screws and Pedicle Screws in Transforaminal and Posterior Lumbar Interbody Fusion

Corresponding Author
Dong Hwa Heo
https://orcid.org/0000-0003-1203-4550

Department of Neurosurgery, The Leon Wiltse Memorial Hospital, 437 Gyeongsu-daero, Paldal-gu, Suwon 16480, Korea
Tel: +82-31-240-6281
Fax: +82-31-240-6282
E-mail: spinesurgery@naver.com

Received: February 17, 2018
Revised: February 13, 2019
Accepted: February 14, 2019

Dong Ah Sin[1], Dong Hwa Heo[2]

[1]Department of Neurosurgery, Spine and Spinal Cord Research Institute, Yonsei University College of Medicine, Seoul, Korea
[2]Department of Neurosurgery, Spine Center, The Leon Wiltse Memorial Hospital, Suwon, Korea

Objective: Lumbar cortical screw fixation (CSF), rather than pedicle screw fixation (PSF), has recently been attempted in lumbar interbody fusion. The purpose of our study was to evaluate the biomechanical stability of lumbar CSF using a finite element (FE) model.
Methods: A 3-FE model, including the L1 to S1 levels, was designed to evaluate and compare the biomechanical stability of lumbar CSF and PSF in single-level lumbar interbody fusion at L4–5. Cortical or pedicle screws were inserted bilaterally, and posterior lumbar interbody fusion (PLIF) and transforaminal lumbar interbody fusion (TLIF) were modeled at L4–5, respectively. We compared the stability of CSF to that of PSF in these 2 different anatomic variations of PLIF, as well as in TLIF.
Results: Lumbar CSF showed less stability than PSF in PLIF when the midline posterior ligaments were not preserved, but demonstrated similar stability when the ligaments were preserved. The range of motion (ROM) at the treated level in CSF was larger than that observed for PSF, in all PLIF and TLIF models. Furthermore, the ROM in the posterior ligament-sacrificing PLIF with CSF model was larger than the ROM in the posterior ligament-preserving PLIF with CSF or PSF model.
Conclusion: Based on our FE analysis, the stability of CSF is comparable to that of PSF in PLIF and TLIF when the midline posterior ligaments are preserved.

Keywords: Finite element analysis, Biomechanics, Lumbar

INTRODUCTION

Of the various lumbar interbody fixation techniques, pedicle screw fixation (PSF) is the standard and most commonly used method.[1,2] However, PSF requires wide dissection and retraction of the posterior muscular structures. Excessive dissection and retraction of the back muscles can cause unnecessary injury and atrophy of the muscles, resulting in significant postoperative back pain. Recently, percutaneous lumbar PSF has been introduced to minimize the skin incision and injury of the posterior muscular structures.[3,4] Additionally, cortical screw fixation (CSF) using a cortical bone trajectory rather than PSF has been attempted in lumbar interbody fusion.[5-9]

Since lumbar CSF utilizes a mediolaterosuperior cortical bone trajectory, this CSF technique may maximize the contact between screw and cortical bone.[10] And, this cortical technique has the same stability as traditional PSF in one cadaveric study.[1] The cortical bone trajectory reduces posterior muscle dissection and injury than traditional PSF techniques.[1,10] However, the biomechanical stability and strength of CSF have not been adequately clarified. Therefore, in the present study, we aimed to compare the biomechanical stability of CSF and PSF in lumbar interbody fusion under different loading conditions by using a finite element (FE) model that utilized computed tomography (CT)-matched properties that reflect the cortical bone structures.

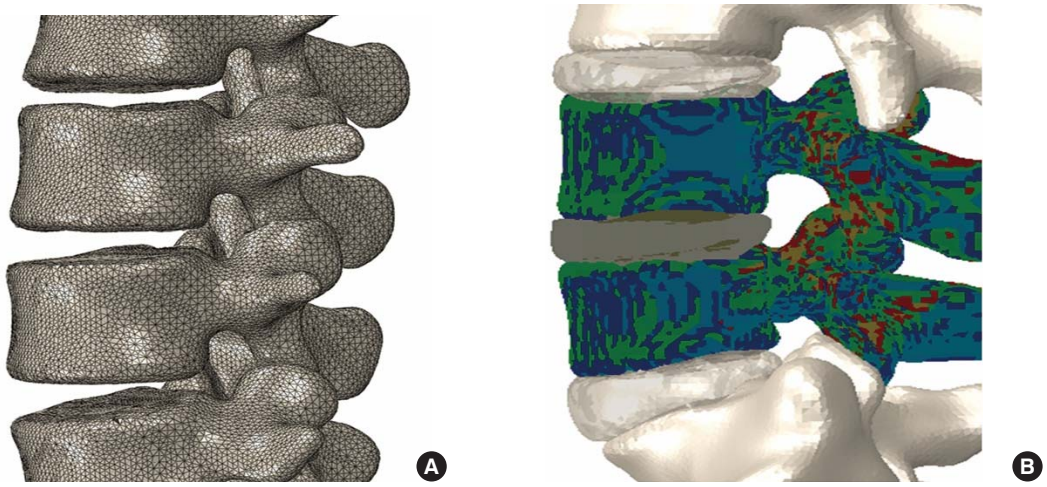

Fig. 1. (A) Lumbar model with a 4-noded tetrahedral element created using Abaqus (Dassault Systèmes, Paris, France). (B) Three-dimensional model showing variation of the element properties.

Table 1. Material properties of the finite element model

Component	Material model	Low Young's modulus (MPa)	Transition strain (%)	High Young's modulus (MPa)	Poisson ratio	Cross section (mm^2)
Cortical bone	Linear elastic	10,000	-	-	0.2	-
Anterior longitudinal ligaments	Nonlinear	7.8	12	20	-	63.7
Posterior longitudinal ligaments	Nonlinear	10	11	50	-	20
Ligamentum flavum	Nonlinear	15	6.2	19	-	40
Facet capsule	Nonlinear	7.5	25	33	-	60
Interspinous ligament	Nonlinear	8	20	15	-	40
Supraspinous ligament	Nonlinear	10	14	12	-	30
Intertransverse ligament	Nonlinear	10	18	59		3.6
Screws and rods	Linear elastic	110,000	-	-	0.3	-
Polyether ether ketone cages	Linear elastic	4,000	-	-	0.3	-

Cancellous bone (Materials matched, $\rho = 1.067$ HU+131 [g/cm^3], E = 0.09882, $\rho^{1.56}$ [megapascal, MPa]), Nucleus pulposus (Mooney-Rivlin, C10 = 0.12, C01 = 0.09, D1 = 1), and Annulus fibrosus (Mooney-Rivlin, C10 = 0.56, C01 = 0.14, D1 = 1).

MATERIALS AND METHODS

1. FE Models

A 3-dimensional (3D) nonlinear FE model of the lumbar spine from the L1 to S1 levels was developed (Fig. 1A).[11] To develop the model geometry, a high-resolution CT scan (1.0-mm thickness) of a healthy 24-year-old man with no spinal disease was performed after obtaining his consent. We imported the DICOM data into Mimics (Materialise, Leuven, Belgium), which generated a 3D model. Thereafter, the 3D spine model was imported into Hypermesh (Altair, Troy, MI, USA), which generated an FE mesh for analysis. Abaqus (Dassault Systèmes, Paris, France) was used to simulate surgical scenarios using the spine model. The FE model comprised five lumbar vertebrae, 1 sacrum, 5 intervertebral discs, 2 endplates for each level, and 7 spinal ligaments, including the anterior longitudinal, posterior longitudinal, intertransverse, ligamentum flavum, capsular, interspinous, and supraspinous. Cancellous bone was modeled with tetrahedral elements. We used shell elements with 1-mm thickness for cortical bone, endplates, and facet contact surfaces, while truss elements were used to model ligaments. Surface-to-surface contact was used to simulate interactions between the articulating surfaces of the facet joints. This FE model of an intact spine was validated by comparing with the cadaveric study by previously published FE models[12,13] and Yamamoto et al.[14]

2. Material Properties

The properties of all elements were assigned as listed in Table 1.[11,15-21] Linear elasticity was applied to bone and cartilaginous structures. The material properties of cancellous bone were represented in Mimics using a numerical expression of the relationship among CT gray value, mass density, and Young's modulus (Fig. 1B). We used a region-specific elastic modulus for the best simulation of CSF. The nonlinear behavior of intervertebral discs was modeled to be hyper-elastic.[11,15-21] The parameters of the Mooney-Rivlin formulation were used, as suggested in a previous study.[11,15-21] The spinal ligaments were designed as bilinear, with specific yield strain and stress values. Young's modulus for screws/rods and polyether ether ketone (PEEK) cages were assumed to be 110,000 and 4,000 MPa (megapascal), respectively.

3. Lumbar Interbody Fusion Models

We used posterior lumbar interbody fusion (PLIF) and transforaminal lumbar interbody fusion (TLIF) models at L4–5 (Fig. 2). Surgical scenarios were created according to the type of screw fixation, interbody fusion, and posterior ligaments (PL) preservation. Six scenarios were simulated in this study: (1) PL-sacrificing PLIF with PSF, (2) PL-sacrificing PLIF with CSF, (3) PL-preserving PLIF with PSF, (4) PL-preserving PLIF with CSF, (5) TLIF with PSF, and (6) TLIF with CSF. To simulate PLIF, partial laminectomy was performed bilaterally at the L4 lamina, while preserving the bilateral L4–5 facet joints by more than 50%. Thereafter, the whole intervertebral disc was removed and replaced with two PEEK cages at L4–5 (Fig. 2). Experimental definition of PL-preserving PLIF model is removal of bilateral inferior articular process, bilateral laminotomy without sacrificing of spinous process and posterior ligamentous structures. In contrast, experimental definition of PL-sacrificing PLIF is removal of bilateral inferior articular process, and subtotal laminectomy. To simulate TLIF, right-side hemilaminectomy and unilateral total removal of the right L4–5 facet joint were performed. A single cage was inserted tangentially at L4–5 (Fig. 2). In both PLIF and TLIF, the cages were bonded to the cortical bone with a tie contact condition to simulate successful fusion. The PLs, including the interspinous and supraspinous, were optionally removed in the PLIF models. Thereafter, we applied four simulated cortical screws or four pedicle screws in each

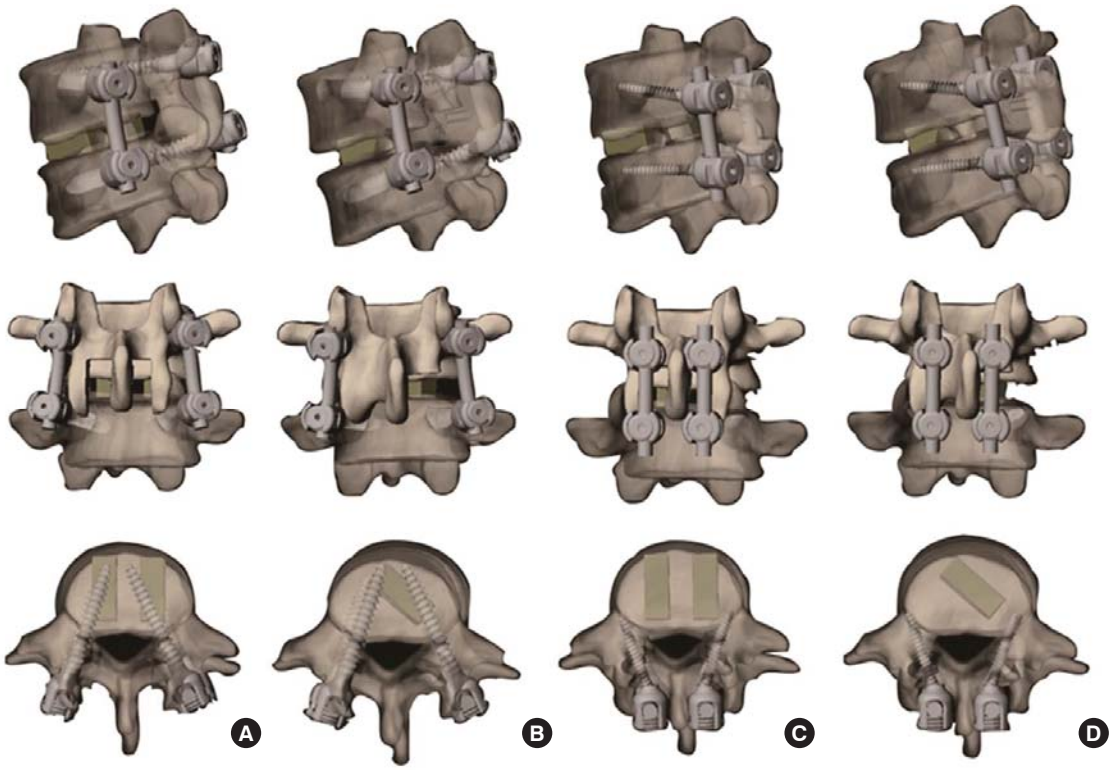

Fig. 2. Experimental setup of different lumbar interbody fusion models at L4–5. (A) Posterior lumbar interbody fusion (PLIF) with pedicle screw fixation (PSF). Posterior ligaments were optionally removed. (B) Transforaminal lumbar interbody fusion (TLIF) with PSF. (C) PLIF with cortical screw fixation (CSF). Posterior ligaments were optionally removed. (D) TLIF with CSF.

https://doi.org/10.14245/ns.1836030.015

scenario. The cortical screw trajectory was from the inferomedial borderline to the superolateral borderline of the pedicle (Fig. 2). The pedicle screws had an outer diameter of 6.5 mm and length of 45 mm, while the cortical screws had an outer diameter of 4.0 mm and length of 35 mm. The cages were 12 mm in height and 30 mm in length in the TLIF models, and 12 mm in height and 24 mm in length in the PLIF models. This dimensions of the screws and cages which were used in the current study were determined to be commonly used in Korean patients in actual surgeries.

4. Boundary and Loading Conditions

The lower half of the sacrum was completely fixed in all directions. The FE model used 2 different loading conditions. For validation, the model was simulated under the same loading condition that was used in the human cadaveric study by Yamamoto et al.[14] A reference point was created and constrained to the surface nodes of the L1 vertebra for force and torque application in the FE analysis. Pure unconstrained 10-Nm flexion, 10-Nm extension, 10-Nm lateral bending, and 10-Nm torsion moments were applied to the reference point in a stepwise manner. For clinical simulation, a compressive load of 400 N and momentum of 7.5 Nm were applied to the same reference point as the flexion, extension, lateral bending, and torsion moments generated under the compressive preload. To reach the target moment, 10 load steps were applied. The range of motion (ROM) at the endpoint of the loading cycle was calculated and compared with that in the cadaveric model.[14] In the present study, ROM was examined in the 4 above-mentioned motions generated in each of the 6 surgical scenarios. In addition, intradiscal

Table 2. Comparison of range of motion between the current finite element model and the cadaveric study by Yamamoto et al.[14]

Moment	Level	Current study	Yamamoto's study, mean ± SD
Flexion (°)	L1–2	4.6	4.2 ± 0.4
	L2–3	5.4	5.4 ± 0.3
	L3–4	6.7	6.1 ± 0.6
	L4–5	7.4	7.1 ± 0.6
	L5–S1	7.6	7.0 ± 0.6
Extension (°)	L1–2	3.1	2.8 ± 0.3
	L2–3	3.3	3.3 ± 0.3
	L3–4	2.5	2.3 ± 0.2
	L4–5	4.3	4.0 ± 0.5
	L5–S1	4.9	4.8 ± 0.6
Rotation (°)	L1–2	2.1	1.7 ± 0.4
	L2–3	1.7	1.4 ± 0.3
	L3–4	2.3	2.0 ± 0.3
	L4–5	1.5	1.4 ± 0.2
	L5–S1	1.3	1.1 ± 0.2
Lateral bending (°)	L1–2	3.8	3.7 ± 0.1
	L2–3	5.4	5.1 ± 0.4
	L3–4	4.7	4.4 ± 0.3
	L4–5	4.6	4.3 ± 0.4
	L5–S1	4.2	3.9 ± 0.3

SD, standard deviation.

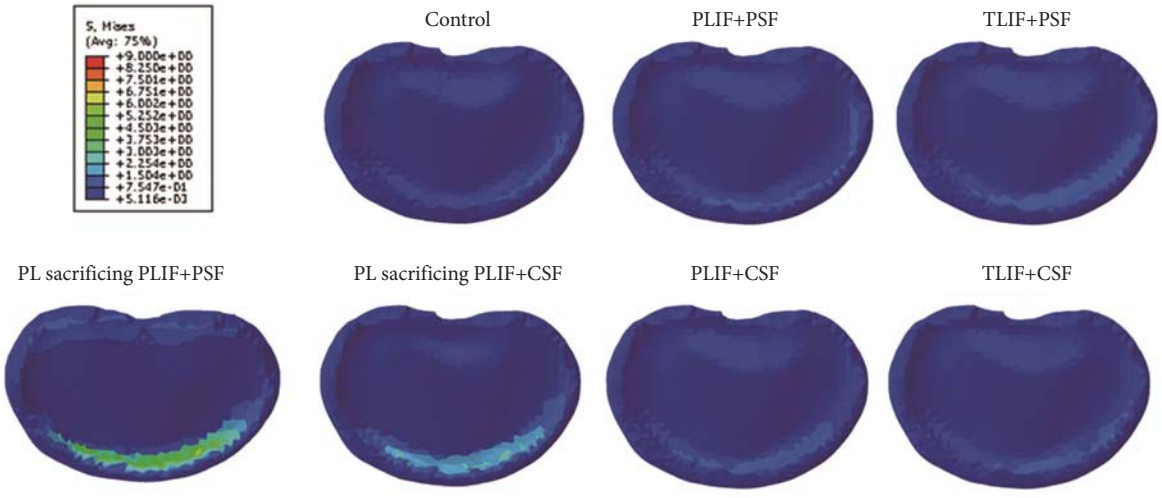

Fig. 3. Von Mises stress at L3–4 after full flexion. Under flexion moment, the largest von Mises stress was observed at the anterior annulus in the PL-sacrificing PLIF model. CSF, cortical screw fixation; PL, posterior ligaments; PLIF, posterior lumbar interbody fusion; PSF, pedicle screw fixation; TLIF, transforaminal lumbar interbody fusion.

Table 3. Range of motion at the treated L4–5 level

	Flexion (°)	Extension (°)	Lateral bending (°)	Rotation (°)
Control	6.40	2.97	1.75	5.48
PLIF with PSF	0.15	0.03	0.12	0.16
TLIF with PSF	0.19	0.16	0.43	0.16
PL-sacrificing PLIF with PSF	0.17	0.03	0.11	0.11
PL-sacrificing PLIF with CSF	0.22	0.23	0.56	0.24
PLIF with CSF	0.21	0.22	0.19	0.23
TLIF with CSF	0.26	0.27	0.40	0.33

PLIF, posterior lumbar interbody fusion; PSF, pedicle screw fixation; TLIF, transforaminal lumbar interbody fusion; PL, posterior ligaments; CSF, cortical screw fixation.

pressure at L3–4 was also measured (Fig. 3).

We compared the stability of CSF with that of PSF in the 2 different anatomic variations of PLIF as well as in TLIF.

RESULTS

1. Model Validation

The FE model of an intact spine was validated before simulating lumbar interbody fusion. ROM in a control model was compared with that in the cadaveric study by Yamamoto et al.[14] (Table 2) and previously published literatures.[12,13] Experimental and loading conditions were identical. Our ROM results were amenable with those of the previous study.[12,13] As shown in Table 2, the obtained data were within 10% of the average values of 10 cadavers tested *in vitro*. The difference was considered to occur due to differences between the subjects used to design the models.

2. Changes in ROM According to the Lumbar Interbody Fusion Model

The ROM at L3–4, L4–5, and L5–S1 was compared under each of the four moments among the six models. At the treated level (L4–5), the ROM of flexion, extension, lateral bending, and rotation was significantly decreased after lumbar interbody fusion, compared with the intact control model (Table 3). ROM at the treated level in CSF was larger than that in PSF, in all PLIF and TLIF models. In particular, ROM in the unilateral facetectomy status (TLIF) with CSF was the largest than another fusion conditions. And, ROM in the PL-sacrificing PLIF with CSF model was larger than that of PL-preserving PLIF with CSF or PSF model (Table 3).

Table 4. Intradiscal pressure at L3–4 after full flexion

Variable	MPa	psi
Control	0.1400	20.31
PLIF with PSF	0.1866	27.06
TLIF with PSF	0.1905	27.63
PL-sacrificing PLIF with PSF	0.2557	37.08
PL-sacrificing PLIF with CSF	0.2104	30.51
PLIF with CSF	0.1871	27.14
TLIF with CSF	0.1819	26.39

MPA, megapascal; psi, pound force per square inch; PLIF, posterior lumbar interbody fusion; PSF, pedicle screw fixation; TLIF, transforaminal lumbar interbody fusion; PL, posterior ligaments; CSF, cortical screw fixation.

3. Changes in Adjacent Intradiscal Pressure According to the Lumbar Interbody Fusion Model

Intradiscal pressure was measured at the center of each intervertebral disc. The absence of PLs significantly elevated the intradiscal pressure at L3–4 in both CSF and PSF (Table 4, Fig. 3). The lowest intradiscal pressure was measured during full flexion in the TLIF with CSF model (26.39 pound force per square inch [psi]), whereas the highest pressure was found in the PL-sacrificing PLIF with PSF model (37.08 psi). The other fusion techniques with PL preservation showed similar results (27.06–27.63 psi).

DISCUSSION

Lumbar interbody fusion has been the standard surgical treatment for lumbar degenerative disease with instability.[22,23] Regardless of surgical technique, the optimal strength of instrumented fixation is important until solid bony fusion occurs. Lumbar instrumentation should provide sufficient strength for stabilization since early instrumentation failure may lead to fusion failure, which can result in postoperative back pain, instability, and kyphosis. Furthermore, an additional salvage operation may be required in some cases with fusion failure.

Although PSF provides sufficient strength and is a very familiar technique for spine surgeons, wide dissection and retraction of the posterior back muscles are demerits that can induce severe muscle atrophy and significant postoperative pain.[24-26] It has been proposed that the preservation of posterior muscle structures is important for the prevention of postoperative back pain and the success of lumbar stabilization.[24] Therefore, minimally invasive techniques have been introduced to preserve the posterior paravertebral muscles, including the multifidus.[27-29]

https://doi.org/10.14245/ns.1836030.015

Because the starting point of lumbar CSF is located more medially than that of PSF, this technique can avoid extensive muscle dissection and retraction.[1] Based on this concept, CSF has been referred to as midline lumbar interbody fusion.

The cortical screw trajectory is from the inferomedial portion to the superolateral portion of the pedicle.[5,6]

CSF not only has a better muscle-sparing effect, but also utilizes screws with a smaller outer diameter and shorter length than those used in PSF.[1] It was reported in one biomechanical cadaveric study that CSF provides approximately the same stability as PSF in TLIF and direct lateral interbody fusion (DLIF).[1] However, that investigation only utilized TLIF and DLIF procedures that preserved the PL, and there was no comparative analysis of PLIF procedures. In the present study, the strength of CSF was weaker than that of PSF in the FE models of PLIF and TLIF. In particular, the strength of conventional PLIF including subtotal laminectomy with CSF was weaker than that with PSF. In addition, we demonstrated similar strength in PLIF with either CSF or PSF when the midline PL structures were preserved. The PL structures, such as the supraspinous and interspinous, are important for lumbar stability.[16,30,31]

We believe that if cortical screws are used in PLIF, the midline PL complex should be preserved for reinforcement of postoperative stability. Furthermore, we do not recommend using cortical screws for the treatment of vertebral fracture with concomitant injury of the PL structures. Based on our study, the biomechanical strength of CSF is slightly weaker than that of conventional PSF.

However, CSF induces less influence at the adjacent levels and, consequently, less increase in intradiscal pressure. We suggested that the trajectory of CSF may be less likely to cause facet joint violation and have less influence on cranial facet joint movement. These effects of CSF may be associated with a less chance of adjacent segment degeneration. However, the effect of CSF on adjacent site degeneration cannot be concluded.

Although we cannot verify the occurrence of iatrogenic muscle injury using this model, the likelihood of injury may be less when CSF is applied. In addition, we believe that CSF has other merits: It can be applied in certain condition, such as those involving polymethylmethacrylate-augmented vertebrae or screw repositioning due to loosening or malposition of pedicle screws.

There are some limitations of our FE model study. First, this study had only a comparative design. Although the strength of CSF was found to be weaker than that of PSF, we cannot know whether CSF can provide sufficient strength until solid fusion. Our FE model also did not have spinal muscular components; therefore, the effects of the lumbar muscular structure could not be evaluated. During CSF or PSF, the muscular structures could be injured, which may affect lumbar stability. However, muscle injury was not reflected in our study. In addition, the cages and screws used in the FE models only had one size. Various situations are possible according to the size of the cage and screw. And, the stress on the screw itself was not measured. In order to obtain a valuable results of screw fixation strength, it is necessary to measure the stress on the screws. Finally, the effects of osteoporosis and osteopenia were not evaluated. Despite these limitations, our study is still valuable since it used an FE model that utilized CT-matched properties that reflect the real bone modulus.

CONCLUSION

In conclusion, based on our FE model analysis, the stability of lumbar CSF was slightly weaker than that of PSF in PLIF and TLIF models. Finally, PL preservation may increase the strength of lumbar CSF. Thus, in lumbar CSF, we recommend that lumbar PL and facet joint should be preserved in order to maintain spinal stability.

CONFLICT OF INTEREST

The authors have nothing to disclose.

REFERENCES

1. Perez-Orribo L, Kalb S, Reyes PM, et al. Biomechanics of lumbar cortical screw-rod fixation versus pedicle screw-rod fixation with and without interbody support. Spine (Phila Pa 1976) 2013;38:635-41.
2. Bevevino AJ, Kang DG, Lehman RA Jr, et al. Systematic review and meta-analysis of minimally invasive transforaminal lumbar interbody fusion rates performed without posterolateral fusion. J Clin Neurosci 2014;21:1686-90.
3. Son S, Lee SG, Park CW, et al. Minimally invasive multilevel percutaneous pedicle screw fixation for lumbar spinal diseases. Korean J Spine 2012;9:352-7.
4. Oppenheimer JH, DeCastro I, McDonnell DE. Minimally invasive spine technology and minimally invasive spine surgery: a historical review. Neurosurg Focus 2009;27:E9.
5. Santoni BG, Hynes RA, McGilvray KC, et al. Cortical bone trajectory for lumbar pedicle screws. Spine J 2009;9:366-73.
6. Mobbs RJ. The "medio-latero-superior trajectory technique":

an alternative cortical trajectory for pedicle fixation. Orthop Surg 2013;5:56-9.
7. Matsukawa K, Yato Y, Kato T, et al. Cortical bone trajectory for lumbosacral fixation: penetrating S-1 endplate screw technique: technical note. J Neurosurg Spine 2014;21:203-9.
8. Mizuno M, Kuraishi K, Umeda Y, et al. Midline lumbar fusion with cortical bone trajectory screw. Neurol Med Chir (Tokyo) 2014;54:716-21.
9. Rodriguez A, Neal MT, Liu A, et al. Novel placement of cortical bone trajectory screws in previously instrumented pedicles for adjacent-segment lumbar disease using CT image-guided navigation. Neurosurg Focus 2014;36:E9.
10. Phan K, Ramachandran V, Tran TM, et al. Systematic review of cortical bone trajectory versus pedicle screw techniques for lumbosacral spine fusion. J Spine Surg 2017;3:679-88.
11. Kim TY, Kang KT, Yoon DH, et al. Effects of lumbar arthrodesis on adjacent segments: differences between surgical techniques. Spine (Phila Pa 1976) 2012;37:1456-62.
12. Park WM, Choi DK, Kim K, et al. Biomechanical effects of fusion levels on the risk of proximal junctional failure and kyphosis in lumbar spinal fusion surgery. Clin Biomech (Bristol, Avon) 2015;30:1162-9.
13. Park WM, Kim K, Kim YH. Effects of degenerated intervertebral discs on intersegmental rotations, intradiscal pressures, and facet joint forces of the whole lumbar spine. Comput Biol Med 2013;43:1234-40.
14. Yamamoto I, Panjabi MM, Crisco T, et al. Three-dimensional movements of the whole lumbar spine and lumbosacral joint. Spine (Phila Pa 1976) 1989;14:1256-60.
15. Chen CS, Cheng CK, Liu CL, et al. Stress analysis of the disc adjacent to interbody fusion in lumbar spine. Med Eng Phys 2001;23:483-91.
16. Goel VK, Monroe BT, Gilbertson LG, et al. Interlaminar shear stresses and laminae separation in a disc. Finite element analysis of the L3-L4 motion segment subjected to axial compressive loads. Spine (Phila Pa 1976) 1995;20:689-98.
17. Lu YM, Hutton WC, Gharpuray VM. Do bending, twisting, and diurnal fluid changes in the disc affect the propensity to prolapse? A viscoelastic finite element model. Spine (Phila Pa 1976) 1996;21:2570-9.
18. Pintar FA, Yoganandan N, Myers T, et al. Biomechanical properties of human lumbar spine ligaments. J Biomech 1992;25:1351-6.
19. Wu HC, Yao RF. Mechanical behavior of the human annulus fibrosus. J Biomech 1976;9:1-7.
20. Polikeit A, Ferguson SJ, Nolte LP, et al. Factors influencing stresses in the lumbar spine after the insertion of intervertebral cages: finite element analysis. Eur Spine J 2003;12:413-20.
21. Shirazi-Adl A, Ahmed AM, Shrivastava SC. Mechanical response of a lumbar motion segment in axial torque alone and combined with compression. Spine (Phila Pa 1976) 1986;11:914-27.
22. Bae J, Lee SH. Minimally invasive spinal surgery for adult spinal deformity. Neurospine 2018;15:18-24.
23. Fay LY, Chang CC, Chang HK, et al. A hybrid dynamic stabilization and fusion system in multilevel lumbar spondylosis. Neurospine 2018;15:231-41.
24. Waschke A, Hartmann C, Walter J, et al. Denervation and atrophy of paraspinal muscles after open lumbar interbody fusion is associated with clinical outcome--electromyographic and CT-volumetric investigation of 30 patients. Acta Neurochir (Wien) 2014;156:235-44.
25. Hartwig T, Streitparth F, Gross C, et al. Digital 3-dimensional analysis of the paravertebral lumbar muscles after circumferential single-level fusion. J Spinal Disord Tech 2011;24:451-4.
26. Mori E, Okada S, Ueta T, et al. Spinous process-splitting open pedicle screw fusion provides favorable results in patients with low back discomfort and pain compared to conventional open pedicle screw fixation over 1 year after surgery. Eur Spine J 2012;21:745-53.
27. Dickerman RD, Reynolds AS, Tackett J, et al. Percutaneous pedicle screws significantly decrease muscle damage and operative time: surgical technique makes a difference! Eur Spine J 2008;17:1398.
28. Foley KT, Gupta SK, Justis JR, et al. Percutaneous pedicle screw fixation of the lumbar spine. Neurosurg Focus 2001;10:E10.
29. Kang MS, Park JY, Kim KH, et al. Minimally invasive transforaminal lumbar interbody fusion with unilateral pedicle screw fixation: comparison between primary and revision surgery. Biomed Res Int 2014;2014:919248.
30. Bresnahan L, Ogden AT, Natarajan RN, et al. A biomechanical evaluation of graded posterior element removal for treatment of lumbar stenosis: comparison of a minimally invasive approach with two standard laminectomy techniques. Spine (Phila Pa 1976) 2009;34:17-23.
31. Tai CL, Hsieh PH, Chen WP, et al. Biomechanical comparison of lumbar spine instability between laminectomy and bilateral laminotomy for spinal stenosis syndrome - an experimental study in porcine model. BMC Musculoskelet Disord 2008;9:84.

 https://doi.org/10.14245/ns.1836030.015